Proceedings of the 5th WSEAS Int. Conf. on Power Systems and Electromagnetic Compatibility, Corfu, Greece, August 23-25, 2005 (pp117-120)

Lightning current parameters-correlations and derived statistics

ILEANA BARAN
Electrical Power Engineering Department
University Politehnica of Bucharest
Splaiul Independentei 313, Bucharest
ROMANIA

Abstract: - The CIGRE-defined lightning current parameters were replaced by a new set of parameters, slightly different, especially for time-components, and univariate analysis was performed for all the involved random variables. Multivariate frequency distribution of the new set of parameters was also analysed and some practical conclusions related to time to crest and steepness of the current, important for lightning protection applications, are presented.

Key-Words: - Lightning, Stroke current, Crest-value, Time to crest, Steepness, Statistical distribution, Correlations

1 Introduction

The present analysis is based upon a sample of lightning current records available in [1], which includes 98 single and multiple negative downward flashes. A previous analysis of the same sample of current waveshapes (WSH) was performed in [2], leading to a full relation of the statistical distribution of lightning current parameters. Correlation amongst the various parameters has also been examined and subsequently analyzed in [3]. The current parameters related to the front of the WSH – designated as front parameters and represented in Fig. 1, will be here referred as CIGRE parameters. The time-origin of the current's waveshape has been set when the actual current value exceeds 2 kA (I_{TRIG}). The coordinates of the first local extreme point A {T100, I100} serve as the basis to define most of the impulse shape parameters. The two CIGRE parameters T10 and T30 are used to estimate the conventional time-to-crest $T_{c,10}$ or $T_{c,30}$ and the steepness S10 or S30.

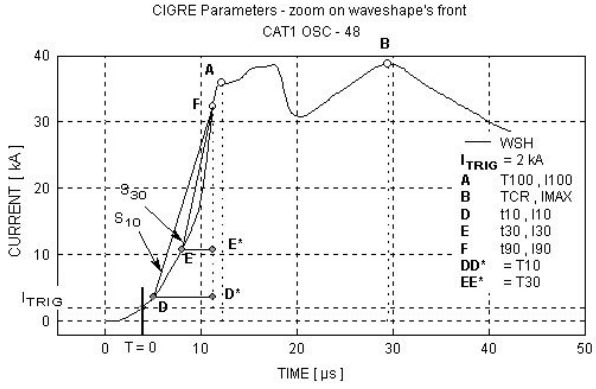

Fig. 1. CIGRE front parameters defined in [1]

Therefore taking into account this previous work our paper will only deal with some aspects of the lightning current shape focusing on the front characteristics, which are of great importance to predict system performances. New parameters were introduced to get a description of the wavefront consistent with the random character of the current waveshapes, [4], [5]. To define the new parameters we used the same characteristic points A to F (located on the WSH) as those used in Fig. 1, but the time coordinates were measured with respect to the first local extreme point on the WSH, i.e. point A{T100-I100} in Fig. 2.

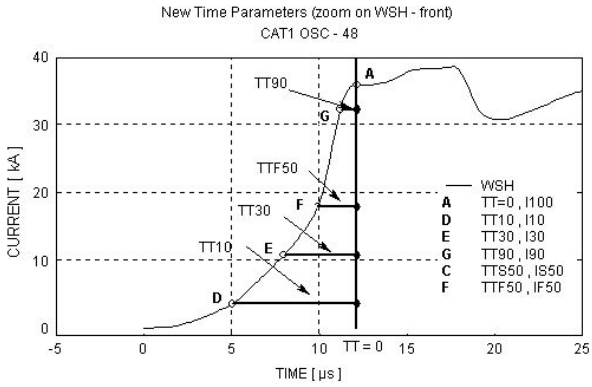

Fig. 2. New front parameters.

The relationships between the new parameters and the CIGRE ones are given in Table 1. As it can be observed the main differences appear for time components.

Table 1

CIGRE parameters	Relationship
T10	= TT10 – TT90
T30	= TT30 – TT90
S10	= 0.8 I100 / (TT10 – TT90)
S30	= 0.6 I100 / (TT10 – TT90)
I100	= I100
IMAX	= IMAX
TAN-G	= DI_MAX

Both the CIGRE-parameters and the new parameters introduced above will be considered further as the components of primary random vectors denoted as $P_{CIGRE} = [P_1, P_2, \cdots, P_m]$ for the CIGRE parameters and

$\mathbf{V} = [V_1, V_2, \cdots, V_p]$ for the new ones. The univariate analysis conducted for the CIGRE-front parameters in [2], produced the results summarized in table2.

Table 2

Parameter	Units	PDF	μ	$\sigma_{\log_{10}}$
T10	[μs]	log	4.5	0.25
T30	[μs]	log	2.3	0.24
S10	[kA/μs]	log	5.0	0.28
S30	[kA/μs]	log	7.2	0.27
I100	[kA]	log	27.7	0.20
IMAX	[kA]	log	31.1	0.21
TAN-G	[kA/μs]	log	24.3	0.26

PDF-Probability Density Function (log standing for lognormal), μ-mean, $\sigma_{\log_{10}}$ -scale parameter for the lognormal distribution.

The results of the univariate analysis conducted in [4] for the new parameters are listed in table 3.

Table 3

Parameter	Units	PDF	μ	$\sigma_{\log_{10}}$
TT10	[μs]	log	7.04	0.161
TT30	[μs]	log	4.714	0.155
TTF50	[μs]	log	3.314	0.160
TT90	[μs]	log	1.57	0.207
TTCR	[μs]	log	10.30	0.333
TTDIM	[μs]	log	2.06	0.191
I 100	[kA]	log	28.90	0.189
IMAX	[kA]	log	33.75	0.210
DI_IMAX	[kA/μs]	norm	10.20	2.823

As it can be seen, all the parameters in tables 2 and 3 are random variables which follow lognormal distributions, except for DI_MAX in table 3 which is normally distributed.

2. Bivariate analysis

Correlation matrix C was computed for all components of the random vector ***V*** but we will give bellow only results pertaining to the front-shape parameters. Zero-order sample correlation coefficients were estimated by the sample coefficient of correlation, (1).

$$r_{i,k} = \frac{1}{n-1}\sum_{j=1}^{n}\frac{(x_i-\mu_i)}{\sigma_i}\cdot\frac{(x_k-\mu_k)}{\sigma_k} = \frac{1}{n-1}\sum_{j=1}^{n} z_i z_k \qquad (1)$$

$\boldsymbol{C} =$

$X_i = \ln V_i$	$\ln(I100)$	$\ln(TT10)$	$\ln(TT30)$	$\ln(TTF50)$	$\ln(TT90)$	$\ln(TTDIM)$	DI_MAX
$\ln(I100)$	1	0.5914 *	0.6049 *	0.4805 *	0.3401 *	0.2335 *	0.7425 *
$\ln(TT10)$		1	0.9248 *	0.7920 *	0.6175 *	0.4981 *	0.0866
$\ln(TT30)$			1	0.9416 *	0.7992 *	0.7071 *	0.0977
$\ln(TTF50)$				1	0.9240 *	0.8793 *	0.0058
$\ln(TT90)$					1	0.9487 *	0.0035
$\ln(TTDIM)$						1	− 0.0521
DI_MAX							1

Marked correlations are significant at p < 0.05

As it can be seen, changing the definition for time-components by measuring them with respect to the first local extreme of the current WSH, had a strong influence on the values of the coefficients of correlation which are increased with regard to those computed for the CIGRE parameters and quoted in [3]. In the following, some of the zero order correlations will be exposed in more details. In Fig. 3 to 6, we plot the bivariate distributions for some pairs of correlated components. With the scattering plot of each sample, we represented the scattering center, the regression lines DREG1 and DREG2, the principal dispersion axes AX1 and AX2, and the concentration ellipses for two different probabilities (ESD-0.3935 and E95-0.950). The characteristics listed above were computed using the theoretical background presented in [5], the inferred parameters in table 3 and the 0-order correlation coefficients from the correlation matrix **C**.

2.1 Correlation DI_MAX÷I100

Correlation reported in Fig. 3 is an important tool that can be used in all lightning protection applications involving the joint effect of the current and current's derivative, such as: predetermination of the risk of failure for the phase insulation under back-flashover conditions, analyze of the surge performance of an earthing system or evaluation of induced voltages.

The characteristics bellow can be used to completely specify the bivariate PDF:

marginal means	$\mathrm{E}[DI\_MAX] = 10.203\,\frac{kA}{\mu s}$; $\mathrm{E}[\ln I100] = \ln(28.9\,\frac{kA}{kA})$
marginal std. deviations	$\mathrm{SD}[DI\_MAX] = 2.823$; $\mathrm{SD}[\ln I100] = 0.435$
correlation coefficient	0.743

The regression lines can be drawn using the equations:

DREG1	$E[DI\_MAX \,\|\, \ln I100] = 10.203 - 4.818 \ln \frac{I100}{28.9}$
DREG2	$E[\ln I100 \,\|\, DI\_MAX] = \ln(28.9) + 0.114\,(DI\_MAX - 10.203)$

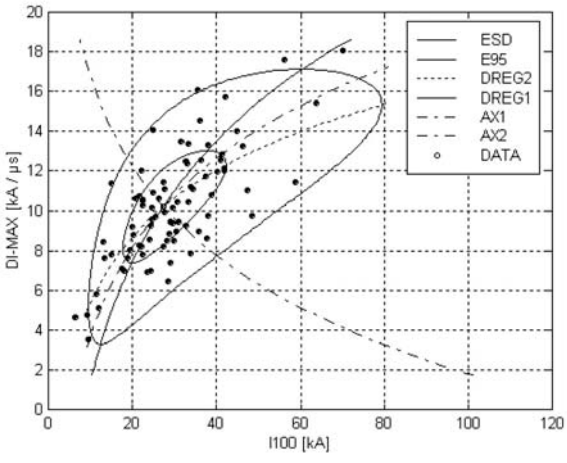

Fig.3 Sample correlation and bivariate lognormal distribution for components *I*100 and *DI_MAX*

2.2 Correlations TT10-TT90 and TT30-TT90

It is also of interest to evaluate the joint behavior of other two pairs of components: {*TT*10, *TT*90} represented in Fig. 4 and {*TT*30, *TT*90} in Fig. 5. The

regression lines equations were obtained following the same rules as mentionned for the previous partial correlation analyzed.

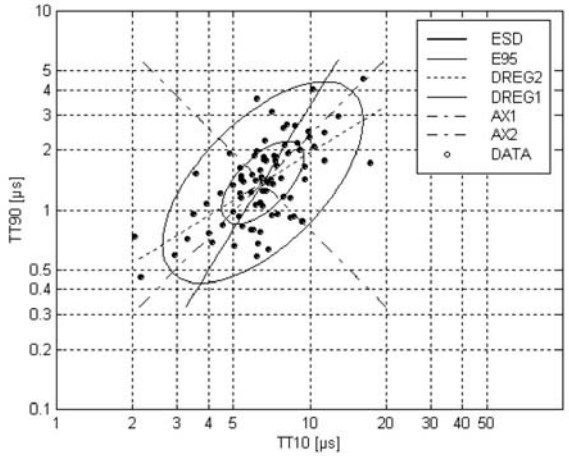

Fig.4 Sample correlation and bivariate lognormal distribution for components *TT*10 and *TT*90

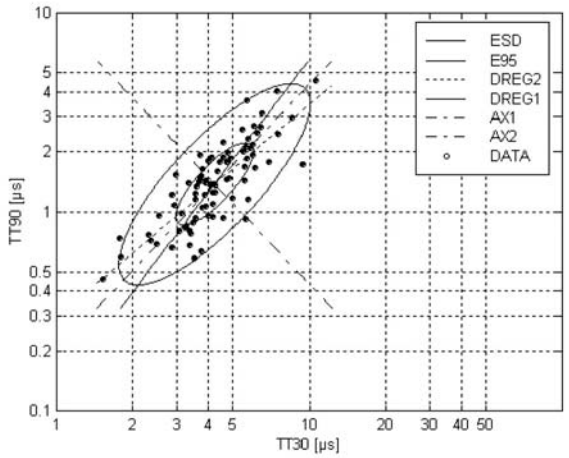

Fig.5 Sample correlation and bivariate lognormal distribution for components *TT*30 and *TT*90

3. Comparison with CIGRE parameters

Having established with reasonable confidence the distributions (PDF) associated with the random vector's **V** components, attention can now be turned to the more difficult problem of finding a suitable distribution for the conventional front duration $T_{f,10}$=T10/0.8 or $T_{f,30}$=T30/0.6. At this purpose, joint probability density functions in figures 4 and 5 can be used. According to table 1 the CIGRE parameters T10 and T30 can be obtained using components *TT*10, *TT*30 and *TT*90, each of the two CIGRE parameters being defined as functions of pairs of correlated random variables having a joint density function (Fig. 4 and Fig. 5). According to the previous results, components {*TT*10, *TT*90} and {*TT*30, *TT*90} are joint log normally distributed, following the bivariate distribution given by:

$$f(x_i,x_j)=\frac{1}{2\pi\sigma_{\ln x_i}\sigma_{\ln x_j}\sqrt{1-\rho^2_{\ln x_i \ln x_j}}}\frac{1}{x_i x_j}\cdot\ldots$$

$$\ldots\cdot\exp\left\{-\frac{1}{2\left(1-\rho^2_{\ln x_i \ln x_j}\right)}\left[\Psi^2_{x_i}-2\rho_{\ln x_i \ln x_j}\Psi_{x_i}\Psi_{x_j}+\Psi^2_{x_j}\right]\right\}$$

$$\text{where:}\quad \Psi_{x_{i(j)}}=\frac{\ln x_{i(j)}-\mu_{\ln x_{i(j)}}}{\sigma_{\ln x_{i(j)}}} \tag{2}$$

In (2), variables x_i and x_j will be the pairs $\{TT10, TT90\}$ or $\{TT30, TT90\}$.

The new random variable defined by :

$$\Delta = x_i - x_j \tag{3}$$

will have the probability distribution function

$$g(\Delta)=\int_0^\infty f(x_i,\Delta+x_i)\,dx_i \tag{4}$$

obtained through a bivariate transformation briefly explained in the following. In 2D a transformation $u=g(x,y), v=h(x,y)$ maps a region $R=I_x\times I_y$ of points in the *xy* plane into a region $S=I_u\times I_v$ of points in the *uv* plane. If the Jacobian of the transformation is never zero over *R* there is a unique inverse transformation

$$x=G(u,v), y=H(u,v) \tag{5}$$

and the density of (*u*,*v*) is given by:

$$\gamma(u,v)=f(G(u,v),H(u,v))\left|\frac{\partial(x,y)}{\partial(u,v)}\right| \tag{6}$$

Knowing the joint density function for variables *xy* , we find the joint density function for variables *uv* and consequently the univariate density functions for each of the variables *u* or *v* as marginal distributions:

$$g_1(u)=\int_{I_v} f(G(u,v),H(u,v))\left|\frac{\partial(x,y)}{\partial(u,v)}\right|dv \tag{7}$$

$$g_2(v)=\int_{I_u} f(G(u,v),H(u,v))\left|\frac{\partial(x,y)}{\partial(u,v)}\right|du$$

Unfortunately the integral in (7) cannot be analytically solved insofar as the authors are aware, although it can be estimated using numerical methods. To obtain the main statistical values (mean and standard deviation) in order to compare them with the corresponding ones reported in [2], the following relations are used:

$$M[\Delta]=\int_0^\infty \Delta\, g(\Delta)\,d\Delta \quad \sigma^2[\Delta]=\int_0^\infty (\Delta-M[\Delta])^2\, g(\Delta)\,d\Delta \tag{8}$$

As the probability density functions of *T*10 and *T*30 are obtained through numerical integration, the differences with respect to the lognormal distributions estimated in [2] can be judged with the help of the values for the mean, standard deviation and p-quantiles for both PDF-s (see table 4), where they can be directly compared with the corresponding estimations given in [2]. Differences are important mainly for the dispersion and consequently for the 5% and 95% quantiles.

The resulting cumulative distribution functions (CDF) for *T*10 and *T*30 are represented in Fig. 6 together with

the sample distribution functions (SDF) and the confidence limits computed with the Lilliefors test for normality, [4].

Table 4

	Statistic	CIGRE [μs]	New CDF [μs]	Difference [%]
*T*10	Mean	5.31	5.41	-1.90
	STD	3.33	2.26	32.10
	5% - quantile	1.80	2.48	-37.78
	95%-quantile	11.30	9.75	13.70
*T*30	Mean	3.03	2.94	2.97
	STD	1.81	1.13	37.57
	5% - quantile	1.80	1.45	19.44
	95%-quantile	5.80	5.08	12.41

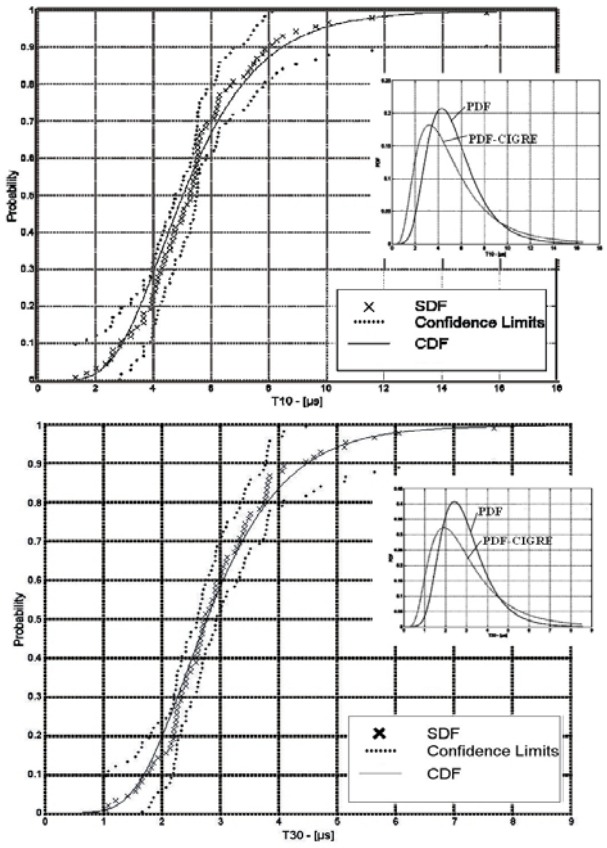

Fig.6 Comparison between the sample (SDF) and the computed cumulative distribution function (CDF)

On the same figure we represented the probability density functions (PDF) for the original CIGRE lognormal distribution and the computed one (with ecuation (7)), to emphasize the differences.

Another interesting result was obtained by re-evaluating the steepness S10 and S30. The steepness (or rate-of-rise) was defined in [1] as:

The definition for the stepness, or rate-of-rise is:

$$S_{10} = \frac{I90 - I10}{TT10 - TT90} = \frac{0.8 \cdot I100}{TT10 - TT90} \qquad (9)$$

$$S_{30} = \frac{I90 - I30}{TT30 - TT90} = \frac{0.6 \cdot I100}{TT30 - TT90}$$

The variables *I*100, *TT*10, *TT*30 and *TT*90 are lognormal and strongly correlated as it can be seen from (3). Consequently, the distribution for the random variable "steepness" in (9), can be obtained using the same rules as those used for the bivariate transformation, extended for four correlated variables. The results are reported in figure 7 and table 5.

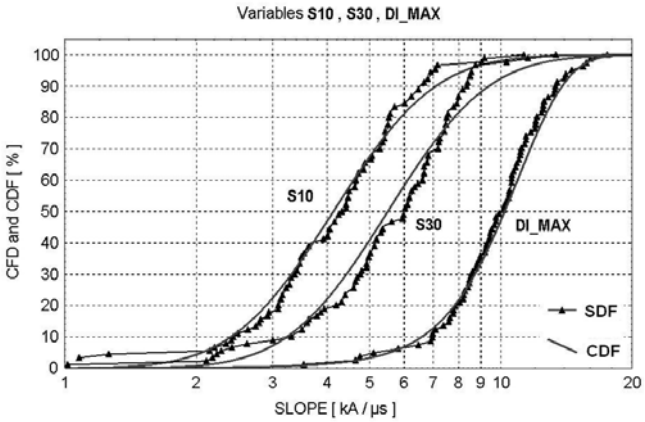

Fig. 7 Sample and computed cumulative distribution functions for steepness S10 and S30. Sample and cumulative distribution for component DI_MAX.

Table 5

	Statistic	CIGRE [kA/μs]	NEW [kA/μs]	Difference [%]
*S*10	Mean	**6.20**	4.51	27.26
	5% - quantile	1.73	2.06	-19.07
	50%-quantile	5.00	4.13	17.40
	95%-quantile	14.44	8.26	42.79
*S*30	Mean	8.73	6.00	31.27
	5% - quantile	2.59	2.77	-6.95
	50%-quantile	7.20	5.50	23.61
	95%-quantile	20.01	10.92	45.43

4. Conclusions

This paper use the new set of parameters introduced in [4] to compute probability density functions for conventional front duration and steepness of the lightning current waveshape. Comparisons are made to the original distributions and differences are analysed.

References

[1] K. Berger, Wissenshaftlicher Bericht über die Blitzforschung auf dem San Salvatore (1963...1971), *8702 Zollikon*

[2] R. B. Anderson, Lightning parameters for engineering application, *Electra*, N°69, 1980

[3] K. Berger, R. B. Anderson, H. Kröninger: Parameters of lightning flashes, *Electra*, Nº41, 1975

[4] Ileana Baran , D. Cristescu, New contribution to the study of lightning current's parameters- Part 1, *Rev. Roum. Sci. Techn.-Electrotechn. et Energ*., 45, Nº4, p. 585-597, Bucarest, 2000

[5] Ileana Baran, New contribution to the study of lightning current's parameters- Part II", *Rev. Roum. Sci. Techn.-Electrotechn. et Energ*., 46, Nº2, Bucarest, 2002